

# Low-Cost Method for Effective Conductivity Improvement of Additively Manufactured All-Metal Waveguide Components

Jakub Sorocki<sup>#</sup>, Ilona Piekarz<sup>#</sup>, Michal Baranowski<sup>§</sup>, Adam Lamecki<sup>§</sup>, Alberto Cattenone<sup>\*</sup>, Stefania Marconi<sup>\*</sup>, Gianluca Alaimo<sup>\*</sup>, Nicolo Delmonte<sup>^</sup>, Lorenzo Silvestri<sup>^</sup>, Maurizio Bozzi<sup>^</sup>

<sup>#</sup> Institute of Electronics, AGH University of Krakow, Poland

<sup>§</sup> Department of Microwave and Antenna Engineering, Gdansk University of Technology, Poland

<sup>\*</sup> Department of Civil Engineering and Architecture, University of Pavia, Italy

<sup>^</sup> Department of Electrical, Computer and Biomedical Engineering, University of Pavia, Italy

{jakub.sorocki, ilona.piekarz}@agh.edu.pl

**Abstract** — In this paper, a low-cost method of 3D printed all-metal waveguide effective conductivity improvement is proposed and studied. The approach is a combination of internal surface polishing to reduce the roughness followed by coating a high-conductivity layer through electroplating. Both methods allow to reduce total power losses within the waveguide which are impacted by the conductivity of the metal. A set of mm-wave test vehicles was developed in WR-28 geometry (26.5 GHz to 40 GHz) being a straight and twisted transmission line section along with a narrowband filter to experimentally validate the approach. The models were 3D printed using Powder Bed Fusion out of stainless-steel powder, dry polished using glass microbeads, and then coated with copper. Up to 40% power loss reduction was obtained with respect to raw prints proving the performance of the approach.

**Keywords** — additive manufacturing, all-metal waveguide, conductivity, direct laser sintering, electroplating, filter, polishing, powder bed fusion, surface roughness, mm-wave.

## I. INTRODUCTION

Additive manufacturing (AM) is a process allowing for the fabrication of three-dimensional objects in a layer-by-layer manner. Recently, AM started to be applied for the realization of microwave circuits reducing their cost and weight as well as allowing for shortening fabrication times and fabrication of geometries not possible with traditional machining techniques [1]. Among all the circuits, waveguide structures are very popular to be realized using AM. In literature, there are many examples of waveguide antennas, filters, etc., which were manufactured using a wide range of AM fabrication techniques [2]. Metallic components like waveguides can be realized by using stereolithography (SLA) by printing elements out of plastic and adding a conductive layer to their surface [3]-[4]. Metal-coated plastic waveguides feature many advantages i.e., they feature high-resolution detail, can be rapidly prototyped, and feature a fairly smooth surface. They are however fragile, and the fabrication processes are not commercially available [5]. On the other hand, Powder Bed Fusion (PBF) technologies like Selective Laser Melting (SLM) unlocked the possibility of fabricating all-metal air-filled waveguiding structures with fairly high resolution and

three-dimensional freedom [6]. Those components are well suited for mm-wave applications due to their relatively low power losses. However, the AM metal parts usually have a poor surface finish compared to milled and turned components which leads to higher conductor-related losses as compared to CNC-fabricated counterparts. Moreover, a variety of metallic powders out of which the parts are made are at best only fair electric conductors.

In this paper, we propose a postprocessing scheme of SLM fabricated waveguide components aimed at improving their effective conductivity and thus reducing total power losses. The approach exploits the low-cost surface polishing method introduced in [6] adding a second step to improve the bulk conductivity of the surface through the electroplating process. An experimental study is conducted for a set of mm-wave test vehicles printed using SLM technology out of stainless steel. After dry polishing using glass microbeads in a rotary tumbler and plating a layer of copper, a loss reduction of up to 40% was achieved validating the proposed approach.

## II. EFFECTIVE CONDUCTIVITY VS. TOTAL POWER LOSS

The conductivity of the PBF fabricated components is lower than the used powder's bulk direct current (DC) conductivity, so effective conductivity is used to describe a given trace/slab properties. In general, the effective conductivity  $\sigma_{eff}$  of a metal layer (assuming uniform material, and thickness much higher than the skin depth at the lowest frequency of operation) is a function of the material's bulk conductivity  $\sigma_{DC}$ , RMS roughness of the surface  $R_q$ , and frequency  $f$ :

$$\sigma_{eff} = f(\sigma_{DC}, R_q, f) \quad (1)$$

One of the models that captures quantitatively this relation is the gradient model [7] where the bulk conductivity and standard deviation of the surface profile are utilized to determine the conductivity profile and then frequency dependency. Having the above, one can determine the surface resistivity  $R_S$  of waveguide walls as [8]:

$$R_S = \sqrt{\frac{\omega\mu_0}{2\sigma_{eff}}} \quad (2)$$

where  $\omega$  is the angular frequency and  $\mu_0$  is permeability in vacuum. On the other hand, the total power loss (TPL) of a two-port is calculated as:

$$TPL = 1 - (|S_{21}|^2 + |S_{11}|^2) \quad (3a)$$

which for a well-matched circuit simplifies to:

$$TPL \approx 1 - e^{-2\alpha l} \quad (3b)$$

where  $l$  is the physical length,  $\gamma = \alpha + j\beta$  is the guides' propagation constant while  $\alpha$  and  $\beta$  are attenuation and phase constants, respectively. In the case of an all-metal air-filled waveguide, the total attenuation is due to the conductor-related losses, so  $\alpha = \alpha_c$  which for a rectangular waveguide operating in TE<sub>10</sub> mode equals [8]:

$$\alpha_c = \frac{R_s}{a^3 b \omega \mu} (2b\pi^2 + a^3 k^2) Np/m \quad (4)$$

where  $\mu$  is the intrinsic permeability,  $a$  and  $b$  are broad- and narrow-wall dimensions.

From the above formulas, one can see that the attenuation constant is inversely proportional to the square of effective conductivity, while the total power loss is exponentially proportional to the attenuation constant. This means that even fair improvement of effective conductivity leads to reduction of power losses. Therefore, to minimize TPL of an AM fabricated component, bulk conductivity should be maximized while surface roughness minimized.

### III. EFFECTIVE CONDUCTIVITY VS. TOTAL POWER LOSS

The proposed effective conductivity improvement method was experimentally validated by the fabrication and processing of a set of test vehicles operating within the mm-wave frequency range. The WR-28 geometry (cross-section of 7.11 mm by 3.56 mm, recommended band between 26.5 GHz and 40 GHz) was selected as it is relatively small so the fabrication and postprocessing can be pushed close to their potential limits while it can still be easily measured. Depending on the component type, the impact is seen as either a reduced attenuation constant in broadband transmission line components or as an increased unloaded quality factor, hence reduced in-band losses in narrowband-like filters. Therefore, to include both types, the following components were developed:

- a straight waveguide section having a total length of 100 mm,
- a five wavelength-long 90° twisted waveguide section having a total length of 65 mm,
- a 3D printing optimized 6<sup>th</sup> order bandpass filter (BPF) [9] operating at the center frequency of 38 GHz with 4% bandwidth having a total length of 65 mm. The minimal dimension of the resonator cavity is ~5.6 mm, while the minimal iris opening is ~3 mm.

The final layouts of the above are shown in Fig. 1. Fabrication and polishing were done the very same way as described in detail in [6]. The test vehicles were fabricated with the Powder Bed Fusion technology using the Renishaw AM 400 Selective Laser Melting type system out of Stainless Steel 316L. For the raw prints, the measured average RMS surface roughness  $R_q$  was roughly 7.9  $\mu\text{m}$  in the direction perpendicular to layer arrangement and 6.1  $\mu\text{m}$  parallel to

layer arrangement. The measured DC conductivity  $\sigma_{DC}$  on the other hand was roughly 1 MS/m.

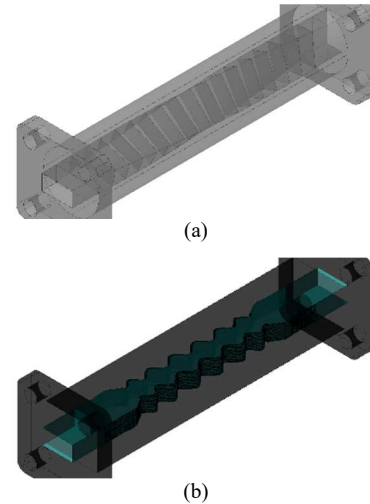


Fig. 1. Isometric view of the final layout of the waveguide twist (a) and narrowband bandpass filter (b).

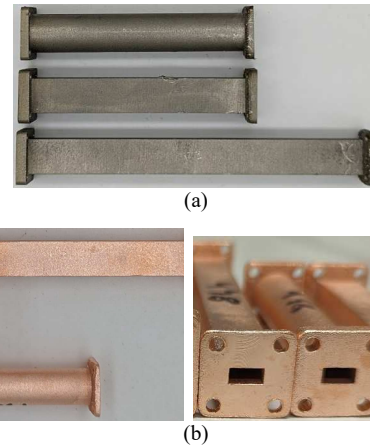


Fig. 2. Photographs of the fabricated test vehicles. Raw stainless-steel SLM-fabricated test vehicles (a). Components after dry tumbling and copper coating (b).

Following, the components were dry tumbled using the Vevor KD-2000, a low-cost jewelry-grade mini rotary tumbler at 50 RPM filled with 300-400  $\mu\text{m}$  large glass microbeads. After the treatment, the measured average RMS surface roughness  $R_q$  was reduced roughly by 18% (6.5  $\mu\text{m}$ ) in the direction perpendicular to the layer arrangement and by 37% (3.9  $\mu\text{m}$ ) parallel to the layer arrangement.

Finally, a copper layer was electroplated on the component's surface. Interestingly, by lowering the resistivity through tumbling, the process of electroplating is improved as it leads to a more even coating along the sides of the component. A generic low-cost setup was used with a cylindrical container filled with electrolyte and copper electrodes inserted accompanied by a magnetic stirrer for better coating, especially inside cavities and channels. The layer was assessed to be roughly 20  $\mu\text{m}$  thick.

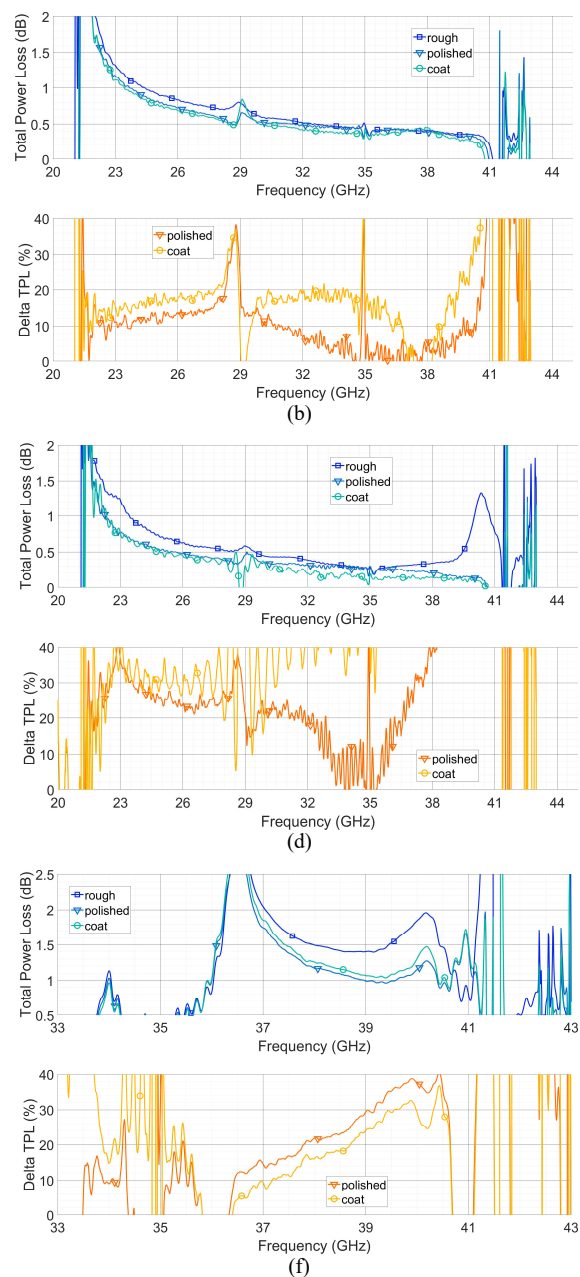
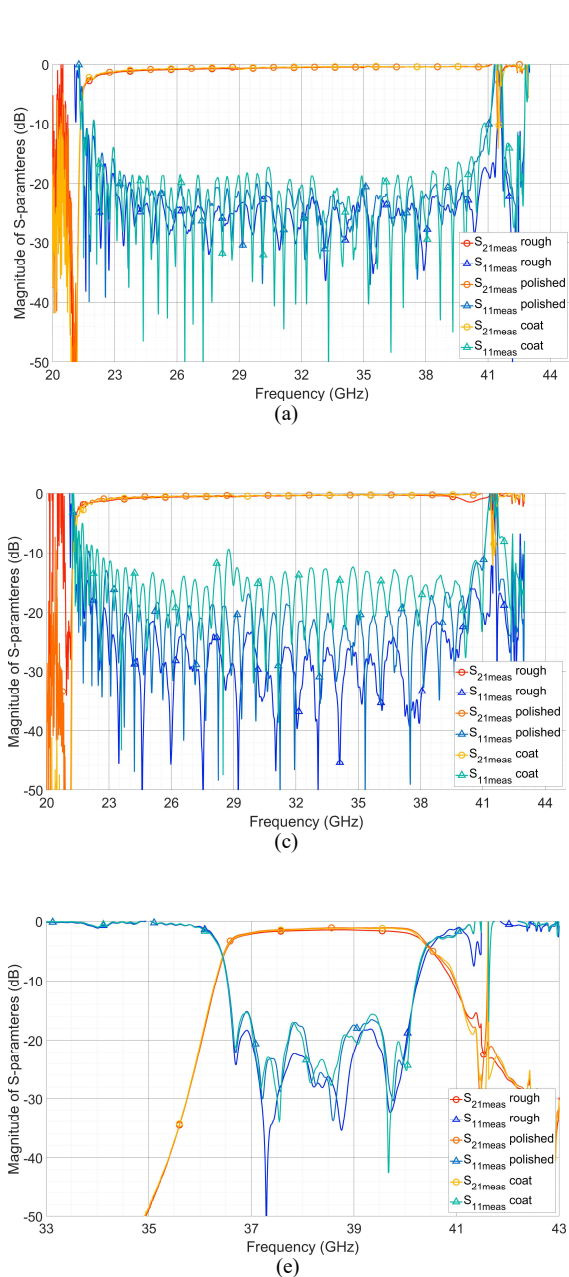


Fig. 3. Measured S-parameters of the SLM-fabricated test vehicles along with the impact of polishing and electroplating on Total Power Loss for straight (a-b), twisted (c-d), and BPF (e-f) WR-28 sized waveguide sections. Delta TPL referenced to raw part TPL.

Scattering parameters of each component were measured at raw printed state, after one 48h polishing cycle and after electroplating to establish the TPL metrics and assess its potential reduction. The Agilent PNA N5224A Vector Network Analyzer was used set at 10 MHz step and 1 kHz of IF bandwidth having the reference plane set at the waveguide flange by calibrating with WR-28 Thru-Reflect-Line cal-kit. Since a relatively small variation in Transmission between processing stages was expected, special care was taken to ensure high repeatability of measurement conditions. The measured frequency response along with calculated TPL and percentage improvement as compared to the raw print is provided in Fig. 3.

Analysis of the above figures allows us to draw the following conclusions. The calculated TPL (delta TPL) data is loaded with high uncertainty as the S-parameter differs by fractions of dB. The BPF case illustrates a cumulative issue of part processing, measurement repeatability, and data uncertainty. The polishing process has a major impact on the effective conductivity of the printed metal providing roughly 10 % to 40% TPL reduction. The electroplating process can further improve conductivity leading to another roughly 5% to 15% TPL reduction. Interestingly, even though the DC conductivity of bulk copper is roughly 60 times higher than bulk stainless steel, the improvement after coating is not that significant. This could be explained by the fact that when

polished, the roughness reduction is more significant concerning current skin depth in stainless steel than in copper for which the skin depth is roughly 7.8 times shallower. Thus, even though the surface is smoother after polishing, the roughness effect is more pronounced after electroplating.

The above observations enable us to formulate further potential ways leading to the improvement of PBF printed metal's effective conductivity. Those are on top of printing out of high-conductivity material. Since metal powder particle size has a direct impact on the roughness, finer powders could be tested. Moreover, since the surface roughness is higher in the direction of propagation due to perpendicular printed layer arrangement, a smaller layer height could be tested so that after laser melting the consecutive lines are ideally unresolvable. Finally, the power, speed, and focus settings of the laser could be fine-tuned for a sharper melting zone. As a result, a smoother surface finish could be obtained right after printing. Later, the above proposed low-cost post-processing schemes could be re-tested to see if the TPL performance can be improved even more.

#### IV. CONCLUSION

The SLM 3D printing technology is very promising for implementing mm-wave components fabrication as it provides sufficient geometry resolution, nevertheless, the inherent rough surface finish possesses a noticeable issue. The above combined with the use of relatively low conductivity powder (e.g. stainless steel) leads to increased surface resistivity of internal walls. As a result, the total power loss within the circuit has increased since for air-filled all-metal waveguides, the conductor loss is its only contributor. Therefore, a combination of a recently developed low-cost internal surface polishing method and the high-conductivity metal coating was proposed as a post-processing scheme and its impact was studied. It was experimentally shown that up to 40% power loss reduction can be obtained proving the usefulness of the approach.

#### ACKNOWLEDGMENT

J. Sorocki and I. Piekarz would like to acknowledge the support of the National Science Centre, Poland, under Grant 2019/34/E/ST7/00342. M. Baranowski and A. Lamecki would like to acknowledge the support of the National Science Centre, Poland, under Grant 2020/39/O/ST7/02897.

#### REFERENCES

- [1] J. R. Montejó-Garai, I. O. Saracho-Pantoja, C. A. Leal-Sevillano, J. A. Ruiz-Cruz, J. M. Rebollar, "Design of microwave waveguide devices for space and ground application implemented by additive manufacturing," in *Proc. Int. Conf. Electromagn. Adv. Appl.*, Turin, Italy, Sep. 2015, pp. 325–328.
- [2] X. He et al., "Additively manufactured "smart" RF/mm-wave packaging structures: A quantum leap for on-demand customizable integrated 5G and internet of things modules," *IEEE Microw. Mag.*, vol. 23, no. 8, pp. 94–106, Aug. 2022.
- [3] M. D'Auria et al., "3-D printed metal-pipe rectangular waveguides," *IEEE Trans. Compon. Packag. Manuf. Technol.*, vol. 5, no. 9, pp. 1339–1349, Sep. 2015.
- [4] J. Sorocki, I. Piekarz, N. Delmonte, L. Silvestri, M. Bozzi, "A Broadband Inline Transition from On-PCB Microstrip to Hybrid Stack-

- up Integrated Additively Fabricated Air-Filled Waveguide," *IEEE Access*, vol. 12, pp. 7884–7895, 2024.
- [5] S. Verploegh, M. Coffey, E. Grossman, Z. Popović, "Properties of 50–110-GHz Waveguide Components Fabricated by Metal Additive Manufacturing," *IEEE Trans. Microw. Theory Techn.*, vol. 65, no. 12, pp. 5144–5153, Dec. 2017.
- [6] J. Sorocki, I. Piekarz, M. Baranowski, A. Lamecki, A. Cattenone, S. Marconi, G. Alaimo, N. Delmonte, L. Silvestri, M. Bozzi, "Low-Cost Method for Internal Surface Roughness Reduction of Additively Manufactured All-Metal Waveguide Components," *IEEE Trans. Microw. Theory Techn.*, early access, 2024.
- [7] G. Gold, K. Helmreich, "A physical surface roughness model and its applications," *IEEE Trans. Microw. Theory Techn.*, vol. 65, no. 10, pp. 3720–3732, Oct. 2017.
- [8] D. M. Pozar, *Microwave Engineering*, 4th ed. Hoboken, NJ, USA: Wiley, 2012.
- [9] M. Baranowski, L. Balewski, A. Lamecki, M. Mrozowski, J. Galdeano, "The Design of Cavity Resonators and Microwave Filters Applying Shape Deformation Techniques," *IEEE Trans. Microw. Theory Techn.*, vol. 71, no. 7, pp. 3065–3074, Jul. 2023.